Nonlinear scattering of near-infrared light for imaging plasmonic nanoparticles in deep tissue

Kentaro Nishida[1,2], Gitanjal Deka[3,4], Nicholas Isaac Smith[5], Shi-Wei Chu[3,6,*], and Katsumasa Fujita[1,2,*]

[1] AIST-Osaka University Advanced Photonics and Biosensing Open Innovation Laboratory, AIST, 2-1 Yamadaoka, Suita, Osaka 565-0851, Japan

[2] Department of Applied Physics, Osaka University, 2-1 Yamadaoka, Suita, Osaka 565-0871, Japan

[3] Department of Physics, National Taiwan University, No. 1, Sec. 4, Roosevelt Rd., Taipei 10617, Taiwan

[4] Department of Physics, The Assam Royal Global University, Betkuchi, Oposite Balaji Temple, Guwahati, Assam 781035, India

[5] Immunology Frontier Research Center, Osaka University, 3-1 Yamadaoka, Suita, Osaka 565-0871, Japan

[6] Brain Research Center, National Tsing Hua University, 101, Sec 2, Guangfu Road, Hsinchu 30013, Taiwan

[*]Corresponding authors: Katsumasa Fujita (fujita@ap.eng.osaka-u.ac.jp) and Shi-Wei Chu (swchu@phys.ntu.edu.tw)

Abstract:

Nonlinear optical microscopy can obtain three-dimensionally resolved images within a specimen by exploiting the nonlinear light-matter interaction between the excitation light and sample. However, the image contrast significantly degrades with increasing observation depth because the emitted signal attenuates during light propagation through layers of the tissue before being detected. To obtain high contrast images from deep tissue, we developed saturated excitation (SAX) microscopy using the nonlinearity of near-infrared (NIR) plasmonic scattering from gold nanoshells and gold nanorods. SAX microscopy selectively detects the nonlinear component from the scattering signal generated by nanoparticle probes located at the center of the focal spot. By using this technique, background signals generated at out-of-focal positions are effectively removed. In addition, emitted signals in the NIR from nanoparticle probes efficiently transmit through biological tissue are ideally suited to image deep parts of the tissue. We experimentally confirmed that scattering intensities from a single gold nanoshell and gold nanorod exhibit nonlinear relations with the excitation intensity of CW laser light at 780 nm and 1064 nm, respectively. We also demonstrated improvements of image contrast and spatial resolution at the depth of 400 μm in a phantom of muscle tissue by selectively detecting the nonlinear scattering signal component from gold nanoshells.

Keywords: Plasmonics, Gold nanoparticle, Near-infrared, Nonlinear, Deep tissue imaging, Super-resolution microscopy

Introduction

Optical microscopy has been utilized to investigate biological samples due to its non-contact and non-invasive capability of live cell imaging. However, to obtain images under thick tissue is still a difficult task to achieve in optical microscopy[1,2]. When imaging in deep tissue, the image contrast significantly degrades because background signals generated at out-of-focal planes overwhelm the signal light from the focus region. To overcome this problem, nonlinear optical responses of contrast probes or sample molecules, such as two-photon excitation of fluorescence[2,3], second harmonic generation (SHG)[4,5] and the saturation of fluorescent excitation[6] have been utilized. Since the nonlinear optical response is induced only at the region where photons are strongly concentrated, a focused laser spot localizes the generation of signal light within a volume smaller than the focal spot. The localization of the signal light provides optical sectioning capability in deep tissue imaging and allows us to obtain a cross-sectional image or a three-dimensional image of thick samples with improved image contrast[1,2,7].

In our previous report, we utilized the nonlinearity of scattering intensity from gold nanosphere probes[8,9] , to obtain high contrast images in deep tissue[10]. We selectively detected the nonlinear scattering signal components from gold nanoparticle probes located within the focal spot by using saturated excitation (SAX) microscopy[11,12] and efficiently imaged the nanoparticle probes at the focal plane of the objective lens by removing out-of-focus signals. Because the nanoparticle probes exhibit strong scattering light through localized surface plasmon resonance[13,14] and high photostability due to stable structure[15], the use of the gold nanoparticle probes allowed us to detect signals even when they were located in deep tissue[10]. In previous experiments[10], we used gold nanospheres with a diameter of 80 nm as contrast probes for SAX microscopy using excitation at 561 nm and confirmed the improvement of image contrast and spatial resolution in imaging the nanoparticle probes under the muscle tissue with a thickness of 200 μm.

In this research, we developed SAX microscopy using the nonlinearity of near-infrared (NIR) scattering from gold nanoshells and gold nanorods, to improve the penetration depth of SAX microscopy. Because the attenuation coefficient of NIR light

for biological tissue is lower than that of visible light[16], both excitation light and scattering light signals can propagate through tissue more efficiently than visible light, which allow us to access deeper parts of the tissue. Gold nanoshells and gold nanorods exhibit the plasmon resonance at NIR wavelength and induce strong scattering of NIR light[17,18]. We experimentally observed that scattering intensity from single gold nanoshells showed the saturation effect by using NIR light with a wavelength of 780 nm and confirmed the improvement of spatial resolution and image contrast in the observation of nanoshell probes at a depth of 400 μm in a phantom of muscle tissue. We also confirmed that the scattering intensity from gold nanorods nonlinearly increased with the increase of excitation intensity at a wavelength of 1064 nm. We previously reported the nonlinearity of scattering intensity from gold nanorods at the excitation wavelength of 785 nm[19]. In this research, the use of gold nanorod probes confirmed the nonlinear scattering at a longer wavelength which can be utilized to achieve observation of deeper parts in a biological tissue.

Observations of nonlinear scattering from single gold nanoshell and gold nanorod

To confirm the nonlinearity of plasmonic scattering from gold nanoshells, we measured the relation between scattering intensity from a single gold nanoshell and excitation intensity. The peak wavelength of plasmon resonance of gold nanoshells is determined by the ratio between the diameter of silica core and the thickness of gold coating[20]. As the thickness of gold coating becomes thinner, the plasmon resonance peak shifts toward a longer wavelength. In our experiment, we used the gold nanoshells with a total diameter of about 160 nm, which are composed of a 120 nm ± 4 nm diameter silica core and 20 nm ± 7 nm thick gold coating (GSLN800-25M, nanoComposix) so that the gold nanoshells have their largest scattering cross-section at the wavelength of ~780 nm by the plasmon resonance. Using this near-infrared resonant wavelength as excitation light is advantageous for observation in the deep part of tissue because of the low scattering efficiency in biological tissue and the low absorption by blood components[21]. The gold nanoshells were dispersed in water purified by using Milli-Q. We measured the extinction spectrum of the gold nanoshells by using spectrophotometer (UV-3600, SHIMADZU), in order to confirm its peak wavelength of the plasmon resonance. As shown in Figure 1a, the extinction spectrum of the gold nanoshells showed the plasmon resonance peak at 771

nm in water. The gold nanoshells were treated by ultrasonic dispersion in order to prevent their aggregation. We placed the gold nanoshells on a glass substrate and immersed them in purified water.

Scattering intensities from single gold nanoshells were measured by laser scanning microscopy. The light source was a continuous-wave (CW) Ti:sapphire laser oscillating at a wavelength of 780 nm (3900S, Spectra Physics), which overlaps with the resonance peak of the gold nanoshells. The scattering signal from an isolated gold nanoshell was detected by a photomultiplier tube (H7710-13, Hamamatsu). A water-immersion objective lens with NA1.0 (LUMPlanFLN, Olympus) was used for excitation and collection of scattering signals from the gold nanoshell.

Figure 1b shows the relation between excitation intensity and scattering intensity from a single gold nanoshell. At an excitation intensity lower than ~3×10^5 W/cm^2, the scattering intensity linearly increased with increasing excitation intensity. However, at the excitation intensity over ~ 3×10^5 W/cm^2, the scattering intensity deviates from the linear slope, indicating the saturation of scattering. This result confirmed that the scattering intensity from gold nanoshells nonlinearly increased with the increase of excitation intensity, which is a needed feature for their use as contrast probes in SAX microscopy.

We also experimentally confirmed the nonlinearity of scattering intensity in single gold nanorods. The resonance peak of gold nanorod is determined by the ratio of lengths between long axis and short axis (aspect ratio). As the aspect ratio of gold nanorod increases, the resonance wavelength shifts toward a longer wavelength[17]. We used gold nanorods with sizes of 67 nm ± 8 nm long and 10 nm ± 2 nm wide (900365-25ML, Sigma Aldrich) in this experiment. The aspect ratio of the gold nanorods is about 6.7. The gold nanorod has the resonance peak at the wavelength of ~1060 nm. Light with a wavelength longer than ~1000 nm exhibits low scattering efficiency and low auto-fluorescence in biological tissue[16]. Thus, the use of near-infrared resonant gold nanorods as contrast probes grants further improvement of the penetration depth in tissue imaging. As shown in Figure 1c, we confirmed that the gold nanorods have a plasmon resonance peak at 1058 nm in water, and the excitation wavelength was therefore chosen to be 1064 nm. Gold nanorods were ultrasonicated to prevent aggregation. We found that scattering signals from gold nanorods were much weaker than that from gold nanoshells and easily covered by background signals caused by reflection from the substrate during the measurement.

Therefore, the gold nanorods were distributed within agarose gel placed onto a glass substrate, instead of directly resting on the glass substrate. The resulting nanorod height above the substrate was sufficient to suppress background light reflections when we measured gold nanorod scattering by using laser scanning microscopy. We used a CW laser oscillating at the wavelength of 1064 nm (Ventus 1064, Laser Quantum) as a light source. The scattering signal from the gold nanorod was detected by an avalanche photodiode (C10508-1, Hamamatsu). A water-immersion objective lens with an NA of 1.0 was used for illumination and observation of the nanorods.

The relation between scattering intensity from a single gold nanorod and excitation intensity is shown in Figure 1d. At excitation intensities below ~5×10^4 W/cm^2, the scattering intensity increased linearly with excitation intensity. When the excitation intensity became larger than ~5×10^4 W/cm^2, the scattering intensity begins to show saturation. However, by further increasing excitation intensity even after the onset of initial saturation, the scattering intensity started to show an increase again at an excitation intensity of ~ 6×10^4 W/cm^2. This phenomenon has been previously described as the reverse-saturation of scattering[9]. These behaviors of saturation and reverse-saturation in the scattering vs excitation intensity relationship were also observed in our previous measurement of scattering intensity from gold nanorod at the excitation wavelength of 785 nm[19]. These results indicate that the nonlinear scattering response of gold nanorods can be induced even at the excitation wavelength of 1064 nm, which is highly beneficial for tissue imaging, and allows the possibility of plasmonic SAX microscopy at this wavelength.

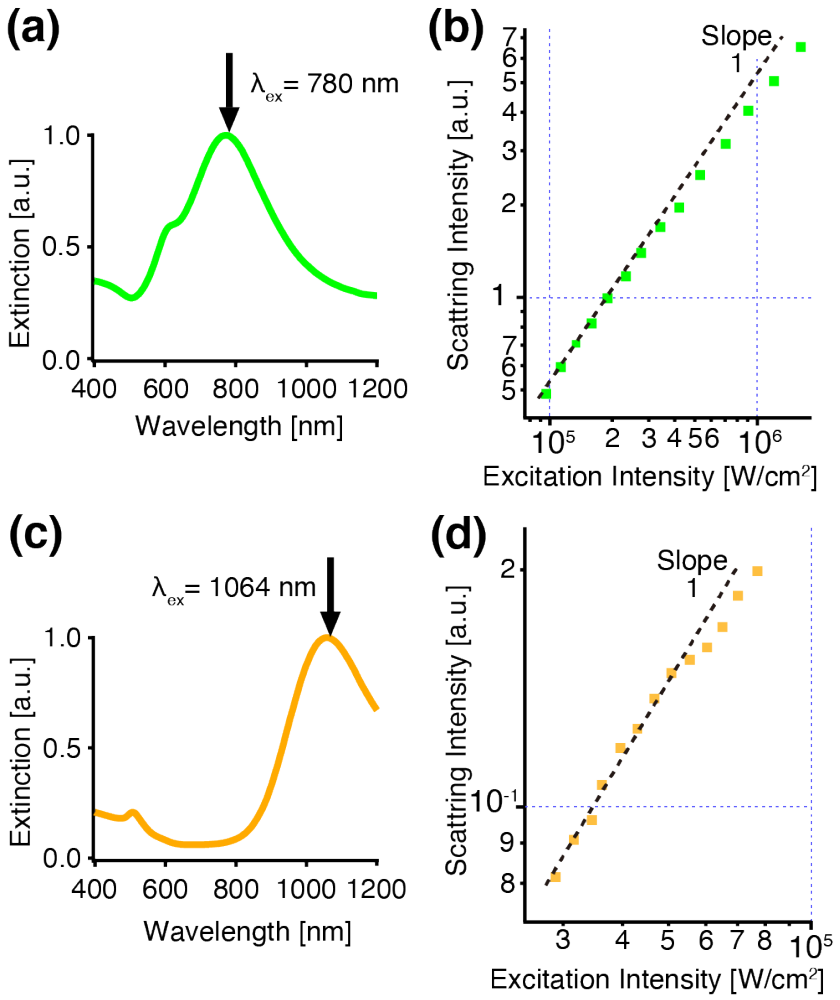

Figure 1. (a)(c) Normalized extinction spectrum of (a) gold nanoshells and (c) gold nanorods. (b)(d) Relations between excitation and scattering intensities from (b) a single gold nanoshell and (d) a single gold nanorod. Both spectra were measured using a spectrophotometer (UV-3600, SHIMADZU). CW laser light with wavelengths of 780 nm and 1064 nm was used to measure the relation between excitation and scattering intensities of gold nanoshells and gold nanorods, respectively.

Extraction of nonlinear scattering from nanoparticles by using SAX microscopy

The nonlinear components in scattering signals from plasmonic nanoparticles can be extracted using SAX microscopy. The setup of a SAX microscope used in our experiments is shown in Figure 2. We used two CW laser sources oscillating at the 780 nm (3900S, Spectra Physics) and 1064 nm (Ventus 1064, Laser Quantum) to excite the gold nanoshell and the gold nanorod at their resonance wavelengths, respectively. We applied temporal modulation to the excitation intensity at a frequency of 10 kHz by using the interference of diffraction beams from two acousto-optic modulators (AOM-402-AF, IntraAction) with a 10 kHz difference in their driving frequencies, which provided stable and low-distortion laser modulation at a single frequency[11]. A part of the modulated laser beam was sampled by a photodetector to detect the reference frequency for a lock-in amplifier (HF2LI, Zurich Instrument). The rest of the laser beam was focused onto the sample through a water-immersion objective lens with an NA of 1.0 and a magnification of 60x (LUMPlanFL N, Olympus) and scanned across the sample in two dimensions using a pair of Galvanometer mirrors. The scattering signals from gold nanoshells and gold nanorods were collected by a photomultiplier tube (H7710-13, Hamamatsu) and avalanche photodiode (C10508-1, Hamamatsu), respectively. The nonlinear components in the modulated scattering signal were detected by the harmonic demodulation technique used for SAX microscopy[11]. The gold nanoshells were placed on a glass substrate and covered by water. The gold nanorods were distributed within agarose gel placed on a glass substrate, as described above.

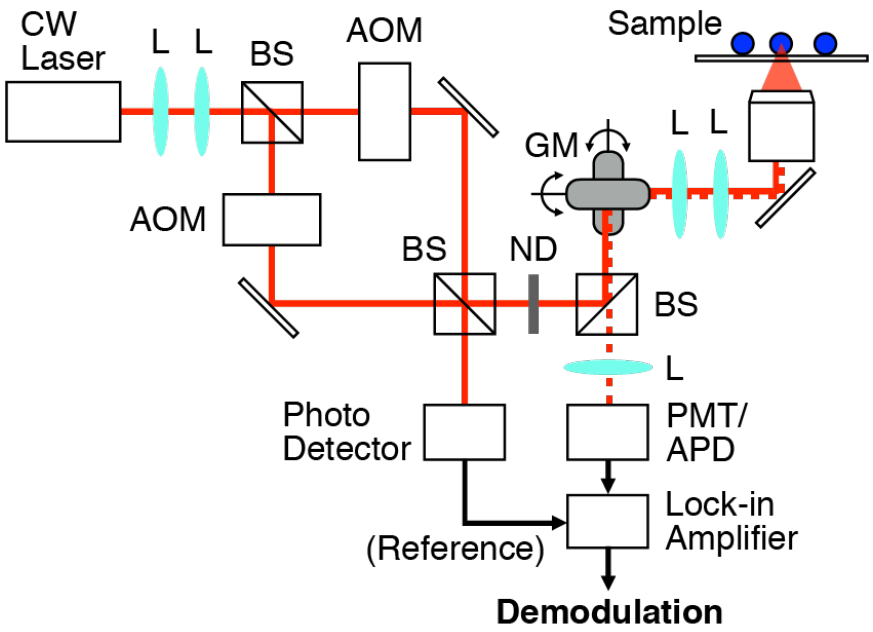

Figure 2. Optical Setup of a SAX microscope (Abbreviations; L: Lens, BS: Beam Splitter, AOM: Acousto-Optic Modulator, ND: Neutral Density filter, GM: Galvanometer Mirrors, PMT: Photomultiplier Tube, APD: Avalanche Photodiode)

Figure 3a shows the relation between the excitation intensity and the demodulated scattering signal from a single gold nanoshell at the fundamental frequency (f = 10 kHz) and the 2nd harmonic frequency ($2f$), respectively. When demodulated at f, the signal intensity follows the excitation intensity nearly linearly, with slight deviation from linearity apparent at excitation intensities above ~6×10^5 W/cm^2. On the other hand, the signal demodulated at $2f$ showed a 2nd order nonlinear relation to excitation intensity when the excitation intensity is higher than ~6×10^5 W/cm^2, indicating 2nd order nonlinear signal was generated by the saturation effect of scattering intensity. The 2nd order nonlinear component is only clearly evident when it is higher than the shot noise component of the scattered light. This means that for low excitation intensities where minimal saturation and therefore minimal nonlinear components occur, we expect to see a demodulated 2nd order intensity which appears to scale with the square root of the excitation intensity (i.e. with a gradient of 0.5 on a log-log graph). This is indeed observed at excitation intensities below ~6×10^5 W/cm^2. When the demodulated signal shows significant nonlinear signals above ~6×10^5 W/cm^2, the demodulated 2nd order scattering intensity transitions to a slope of 2, corresponding to the square of the excitation intensity, consistent with expectations. Figure 3b and 3c show the images reconstructed by

scattering signals demodulated at f and $2f$, respectively. We then compared the intensity profiles of two gold nanoshells in close proximity, in Figure 3d and 3e, respectively. The two-point spatial resolution at Figure 3e was improved compared to Figure 3d. This demonstrates that the nonlinear signal localized at the center of focal spot was selectively detected. This result indicates that the nonlinear component of scattering signal from gold nanoshells was successfully extracted using plasmonic SAX microscopy at 780 nm, which is needed in order to expand the imaging capabilities in tissue samples compared to visible wavelengths. It should be noted that the amount of the nonlinear scattering signal from gold nanoshells also depends on the excitation wavelength. In particular, as the excitation wavelength is closer to the resonance wavelength of the gold nanoshells, the nonlinear scattering signal is more efficiently produced. We experimentally confirmed that the excitation wavelength of 690 nm produces only two times less nonlinear components of scattering signal, compared to the excitation wavelengths of 740 nm or 780 nm which are closer to the resonance peak of the gold nanoshells (See Supporting Information 1). These results implied that the mechanism on the nonlinear scattering of gold nanoshells was related to the plasmon resonance.

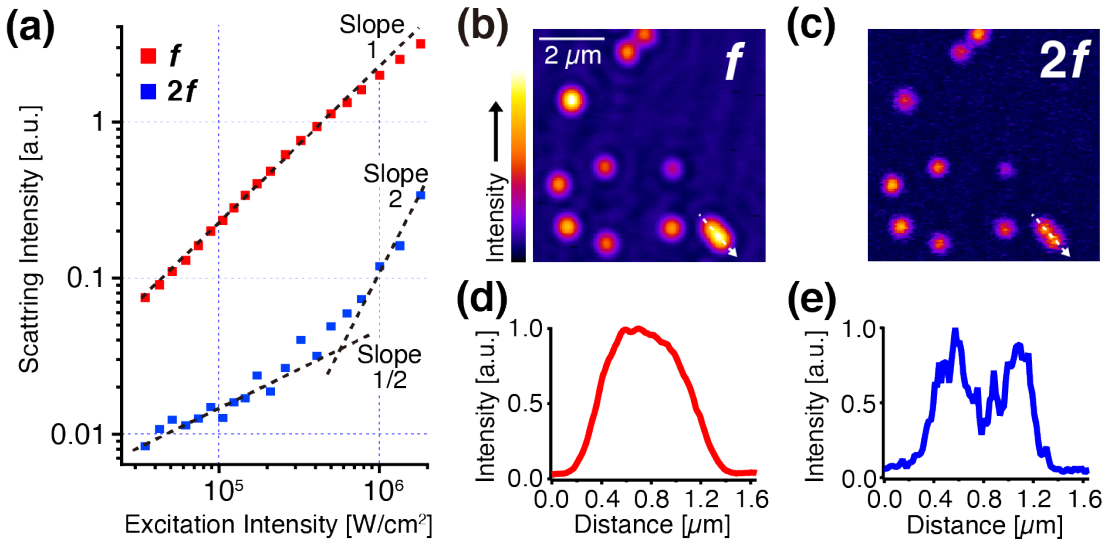

Figure 3. (a) Relation between excitation intensity and demodulated scattering signal from a single gold nanoshell at fundamental frequency (f) and 2nd order harmonic frequency ($2f$). (b) (c) Images reconstructed by demodulated scattering signal from gold nanoshells, at f and $2f$. The excitation intensities of (b) and (c) were 1.1×10^5 W/cm^2 and 1.8×10^6 W/cm^2. (d) (e) Normalized intensity profile at the position of white arrow in (b) and (c), respectively.

We also extracted the nonlinear scattering signals and performed SAX imaging by using gold nanorods at 1064 nm. As described above, the gold nanorods were distributed in the agarose gel. Figure 4a shows the relation between the excitation intensity and the scattering signal intensity from a single gold nanorod demodulated at f and $2f$. Similar to the results with gold nanoshells, the signal demodulated at f showed a nearly linear increase with increasing excitation intensity. At the excitation region above ~5×10^4 W/cm^2 , the signal demodulated at f deviated from the linear slope. At these excitation intensities, the scattering signal demodulated at $2f$ appeared and increased proportionally to the square of the excitation intensity, which indicates the 2nd order nonlinear signal was induced due to the saturation of scattering. Figure 4b and 4c are the images of the gold nanorod in agarose gel reconstructed by scattering signal demodulated at f and $2f$, respectively. In Figure 4b, the image contains background scattering signal generated from optical components and agarose gel, in addition to the scattering signal from the gold nanorod. On the other hand, the background signal was removed in Figure 4c, which shows the image of the gold nanorod with a high image contrast. Since the background

signals do not have nonlinear components, the harmonic demodulation at 2*f* effectively removed the background and highlighted the scattering from the gold nanorod that contains the nonlinear signal due to saturation. Figure 4d shows the line profiles of the image of the gold nanorod in Figure 4b and 4c. The full-width half-maximums (FWHM) of the particle images in Figure 4b and 4c were 658 nm and 480 nm, respectively, indicating the improvement of spatial resolution by SAX microscopy. These experimental results show spatial resolution and image contrast can be improved in imaging of gold nanorods by SAX microscopy using NIR light, and indicate that the technique has a potential to image nanoparticle probes in deep tissue by using NIR light for both excitation and detection.

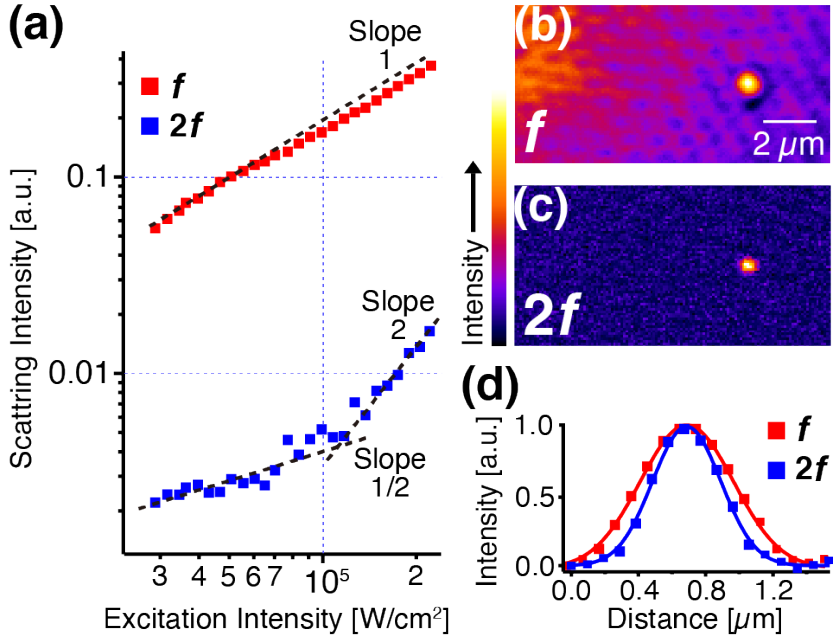

Figure 4. (a) Relation between excitation intensity and demodulated scattering signal from a single gold nanorod at *f* and 2*f*. (b) (c) Images reconstructed by demodulated scattering signal from the gold nanorod, at *f* and 2*f*. The excitation intensities of (b) and (c) were 2.9×10^4 W/cm^2 and 2.2×10^5 W/cm^2, respectively. (d) Normalized cross-sectional profiles of gold nanorod image in (b) and (c)

Improvement of image contrast in deep tissue by using nonlinear scattering from gold nanoshells

After having characterized the saturation behavior and nonlinear component extraction on the nanoparticles, we then performed imaging of gold nanoshell probes through tissue phantoms with SAX microscopy to confirm that the measured behavior can be practically exploited to achieve an improvement in imaging contrast in deep-tissue observations. Figure 5a and 5b show a schematic of the sample conditions and a picture of the sample. We prepared a tissue phantom mimicking muscle tissue in glass bottom dish by using the protocol described by Cubeddu et al.[22]. The tissue phantom was composed of water, agarose gel with a concentration of 1% and Intralipid (I141-100ML, Sigma Aldrich) with a concentration of 1%. The concentration of Intralipid was adjusted so that the transport mean free path in the tissue phantom corresponds to that of animal muscle tissue[23]. The gold nanoshells were randomly distributed in the tissue phantom. We illuminated the gold nanoshells from the bottom of the glass bottom dish through the water-immersion objective lens with an NA of 1.0 and a magnification of 60x (LUMPlanFL N, Olympus). The scattering signal was then collected through the same objective lens. SAX imaging of gold nanoshells was performed at an excitation intensity of 780 nm while gradually changing the height of the objective lens to collect measurements from increasing sample depth. The observation depth shows the distance between the focal plane of the objective lens and the upper surface of the cover glass.

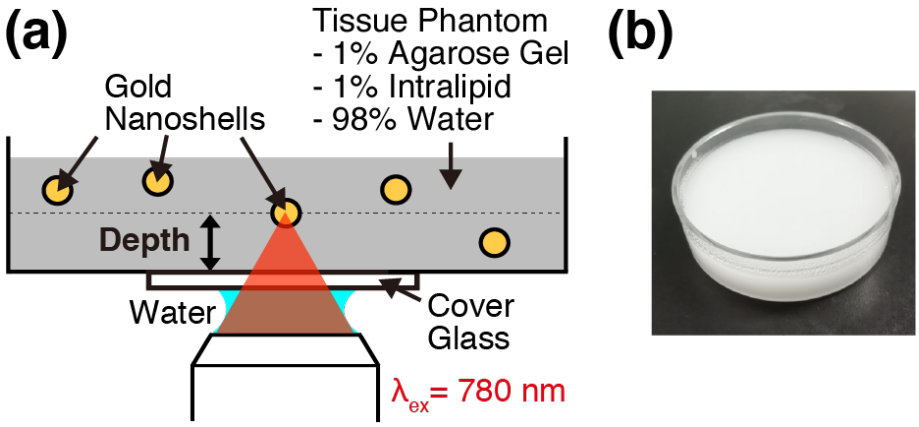

Figure 5. (a) Schematic of the sample condition for the observation of gold nanoshells in a tissue phantom. (b) A photograph of the tissue phantom.

Figure 6a shows the images of gold nanoshells distributed in tissue phantom reconstructed by the signal demodulated at the fundamental (*f*) and the second harmonic frequency (2*f*). Different observation depths of 80 μm, 240 μm and 400 μm in the phantom were observed. At all measured depths, the images reconstructed with demodulation at *f* show strong background due to the light scattering generated from a combination of the tissue phantom itself, gold nanoshells located at out-of-focal positions, as well as optical components. On the other hand, the images reconstructed with demodulation at 2*f* show a much higher image contrast by effectively suppressing these background signals. Since these images are reconstructed by the nonlinear signal, the gold nanoshells with the nonlinear scattering property were selectively imaged with the z-sectioning capability, and the background signal showing a linear response was effectively removed at any depth. These experiments indicate that SAX microscopy can realize high contrast imaging of deep tissue by using NIR light and gold nanoshells as contrast probes.

To quantitatively compare the image contrast at each observation depth, we calculated the signal-to-background ratio (SBR) of images obtained at different observation depths. To obtain the signal value, we averaged the value of 3×3 pixels at the center of particle image. For estimating the background, values of 100×100 pixels at a region without a particle image were averaged. We compared SBRs of images reconstructed by the linear and the nonlinear signal at each observation depth. We also compared the use of the nonlinear SAX signal with the more conventional use of a confocal pinhole, with a pinhole diameter of 1.3 Airy units (i.e. standard confocal scattering microscopy).

Figure 6b shows the relations between SBR and observation depth in linear non-confocal imaging with demodulation at *f* (*f*), linear confocal imaging (Confocal), and nonlinear non-confocal imaging with demodulation at 2*f* (2*f*). At the observation depth of 80 μm, the SBR in confocal image was the highest in these three conditions, indicating the confocal pinhole effectively eliminated the background signal from out-of-focus planes. However, when the observation depth was increased to 160 μm, the SBR of confocal image rapidly decreased, and the SBR in nonlinear non-confocal image (2*f*) then shows the highest SBRs. The reason of this steep decay of SBR in confocal imaging is that the signal photons were significantly scattered during propagation in tissue phantom and not able to be detected through the pinhole. The results at nonlinear imaging (2*f*)

almost perfectly removed the background signal by effectively and selectively detecting the nonlinear signal. Consequently, at observation depths beyond 160 μm, SBRs in the nonlinear image were higher than that of the confocal image. The SBR of linear non-confocal imaging (*f*) were lowest at every observation depth, as expected, because these linear non-confocal images do not have optical sectioning capability. These results indicate SAX microscopy is useful to enhance the image contrast in imaging deep parts of tissue above 100 μm especially, although confocal microscopy can provide better image contrast at shallow observation depths below 100 μm. We thereby confirmed that our technique has the capability to successfully image plasmonic contrast probes in tissue and to improve the image contrast compared to other techniques at observation depths of up to 400 μm in tissue.

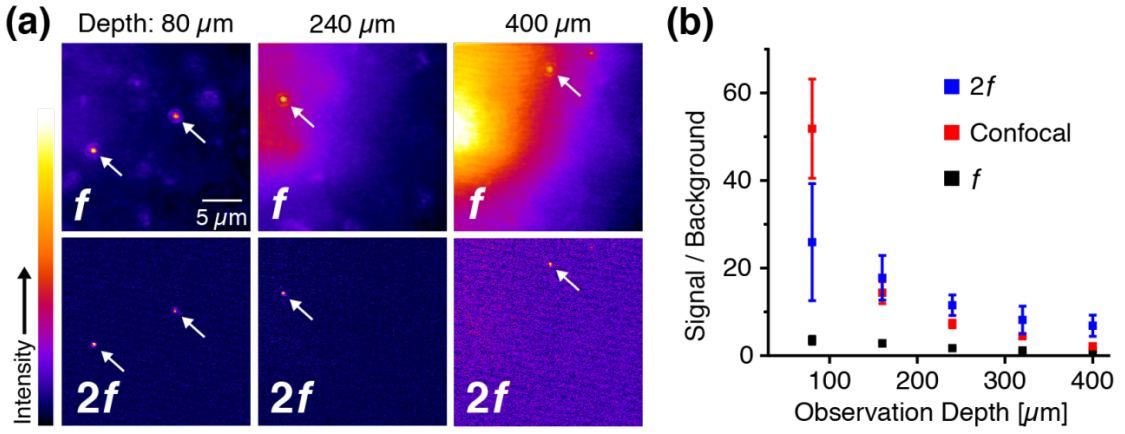

Figure 6. (a) Scattering images of gold nanoshells obtained by SAX microscopy at different observation depths. First column: observation depth of 80 μm, Second column: 240 μm, Third column: 400 μm. Images were reconstructed by demodulating the scattering signal at the fundamental frequency (First row) and 2nd harmonic frequency (Second row). White arrows in each image indicate the positions of gold nanoshells. No confocal pinhole was used in these images. The image dimensions are 256×256 pixels. (b) Relation between signal-to-background ratio and observation depth for image reconstructed by linear signal (Black), image reconstructed by linear signal obtained through 1.3 Airy of confocal pinhole (Red) and image reconstructed by 2nd order nonlinear signal (Blue). N=5. Error bars are 1st standard deviations.

Conclusion & Discussion

We demonstrated saturated excitation (SAX) microscopy using the nonlinearity of NIR plasmonic scattering for high-contrast and background-free imaging in deep tissue. Based on the scattering properties measured in our experiments, we proposed gold nanoshells and gold nanorods that exhibit plasmon resonance in the near-infrared region as contrast probes. We successfully obtained high-contrast images of gold nanoshells even at a depth of 400 μm in a highly-turbid muscle phantom, which is one of the more difficult tissue types for imaging (brain tissue for example has scattering coefficient roughly 1.8 times lower[1]). These experimental results demonstrate the capability of gold nanoshells for contrast probes to detect target molecules, structures or cells in deep tissues.

Our experimental results on the scattering response of gold nanoshells imply that the nonlinearity of plasmonic scattering is a general phenomenon among various structures of plasmonic nanoparticles, taking into account our previous experimental results using gold nanospheres[8,9], silver nanospheres[19] and gold nanorods[19]. However, the degree of nonlinearity in the scattering intensity is different depending on the plasmonic nanoparticle geometry. In the case of gold nanoshells, the increase of scattering intensity showed a smaller deviation from linearity compared to that of other nanoparticle types[9,19]. These results help to understand the physical mechanism of nonlinear scattering. We previously reported that the nonlinearity of plasmonic scattering can be induced by the photothermal effect due to laser irradiation, with calculation results showing that plasmonic scattering of gold nanosphere can saturate as the particle temperature was increased[24]. This photothermal mechanism implies that the absorption cross-section of nanoparticles is more significant to induce the nonlinearity of scattering than the scattering cross-section itself. In the case of our gold nanoshells, while the scattering cross-section shows the maximum at the resonance of 770 nm, the absorption maximum is located at the resonance of ~600 nm. Thus, when gold nanoshells are excited at the resonance of 770 nm, the gold nanoshells are not heated efficiently. This is probably the reason why the gold nanoshell scattering exhibits only a small deviation from linear trend, compared to other nanoparticle types. The small degree of the nonlinearity limits the observable depth of SAX microscopy even though the gold nanoshells have large scattering cross-section in NIR wavelengths region. To improve the penetration depth further, the design of plasmonic nanoparticle structures so that the amount of nonlinear scattering signal is maximized under the excitation of NIR light may be necessary. Also,

the aggregation of the nanoparticles is another factor to affect the image contrast of our technique. Because the aggregation of gold nanoparticles results in the shift of resonance wavelength, the degree of saturation would be different even with using the same excitation wavelength[8] . To prevent the aggregation between nanoparticles, it would be useful to coat nanoparticles with a thin layer of silica that keeps a gap between metallic nanoparticles[25].

We also investigated the scattering property of single gold nanorods that exhibit plasmon resonance at longer wavelengths in the NIR region. By using the nonlinear scattering from the gold nanorods, SAX microscopy using NIR light at the wavelength of 1064 nm was performed. Since the wavelength region between 1000 - 1350 nm shows high transmittance in biological tissues without exciting auto-fluorescence[16], the use of this wavelength region can improve the image contrast and the provide further penetration depth in deep tissue imaging[26–28]. We experimentally demonstrated a capability of optical imaging using 1064 nm light for both excitation and detection, which can expand the penetration depth of optical imaging. However, in our experiment, there was a challenge in signal detection to obtain images of gold nanorod probes in a deep part of the tissue because of the small scattering cross-section of the gold nanorods and the low sensitivity of the photodetector at the NIR region. To increase the scattering intensity of gold nanorods, control of the gold nanorod orientation is one approach, since the gold nanorods scattering cross-section is maximally resonant with 1064 nm incident light when the polarization is aligned with the gold nanorod long axis. In addition, the use of SAX microscopy using differential excitation (dSAX microscopy) [29,30] can be useful to detect nonlinear scattering signal from nanoparticle probes more efficiently. dSAX microscopy can extract an 8-times larger amount of 2nd order nonlinear signal compared to conventional SAX microscopy using harmonic demodulation, which was used in this paper. dSAX microscopy also allows us to use the pulse laser for excitation of probes. The use of a pulse laser can efficiently induce the saturated excitation of plasmonic scattering with the high peak power. The combination of dSAX microscopy and pulsed excitation can improve the penetration depth of our technique further.

It is also interesting in the future to study if our technique allows the use of surfaced enhanced Raman scattering (SERS) from plasmonic nanoparticles as signal light. Since the mechanism of SERS is based on the plasmon resonance, SERS also may show the saturation effect. If so, the signal light from nanoparticle probes can be more

efficiently isolated from the background scattering light by spectral detection, since the wavelength of SERS signal is different from the excitation wavelength.

One of the advantages of our technique is that the transmission efficiency in detection can be improved in imaging at deep tissue by using NIR light as a signal. Even though multiphoton microscopy also uses NIR illumination light to excite fluorescent probe, the wavelength of generated fluorescence signal is shorter than excitation wavelength, which easily attenuates during propagation in tissue layer compared NIR signal light. The detection of nonlinear components using frequency modulation in the NIR region rather than conversion of emitted photons to shorter wavelengths can allow a deeper penetration depth than multiphoton microscopy in deep tissue imaging. Our technique also has the advantage for long-time measurement or repetitive measurements because metallic nanoparticles show photostability. Typically, fluorescence-based nonlinear microscopy suffers from photobleaching during long time measurement because the contrast probes is required to be illuminated with high excitation intensity in order to induce the nonlinear excitation in a deep part of tissue.

Our technique improves the spatial resolution of scattering image beyond the diffraction limit, as well as super-resolution scattering microscopy using coherent anti-Stokes Raman scattering (CARS)[31] and stimulated Raman scattering (SRS)[32]. In our experiment, we improved the spatial resolution in the scattering image from 486 nm to 363 nm for the gold nanoshells placed on glass substrate by detecting the 2nd order nonlinear components of the scattering signal. Even at the observation depth of 400 μm in tissue phantom, the spatial resolution was improved from 580 nm to 392 nm in 2^{nd} order nonlinear images. We also confirmed that the spatial resolution in imaging gold nanorods was improved from 658 nm to 480 nm, by extracting the 2nd order nonlinear signal from the nanorod. It is also possible to improve the spatial resolution by using higher nonlinear components (3^{rd} order, 4^{th} order…) from the scattering signal extracted with demodulation at higher harmonics frequencies (3*f*, 4*f*…). We demonstrated a spatial resolution of 203 nm in imaging gold nanoshells by detecting the 3^{rd} order nonlinear signal (See Supporting Information 2). However, the amount of 3^{rd} order nonlinear signal from gold nanoshells was much lower than that of 2^{nd} order nonlinear signal there is a trade-off between the spatial resolution and the signal amount. Practically, imaging based on the 3rd order nonlinear signal would not reach the observation depths that can be imaged by the 2^{nd} order nonlinear signal

Thermal damage due to the heating of the gold nanoshells can be a problem in tissue imaging by the proposed technique. While it is non-trivial to measure the heat transfer to the surrounding environment, which is the key issue, we did note that during imaging of gold nanoshells distributed in agarose gel, we did not see any movement of gold nanoshells nor deformation of the agarose structure surrounding the gold nanoshells, indicating the local temperature immediately near the particle remained below 85ºC, i.e. the melting point of 1% agarose gel[33]. We did not see evidence of damage, but further research would be of interest. To further probe and optimize temperature effects, differential SAX microscopy[30] and/or optimizing the laser power required for scattering saturation by pulsing or modulating are possibilities.

The technique of deep imaging allows to observe and detect our target in a living specimen. Our method can be useful in applications of cell detection in a living animal, such as locating tumor cells or tracking their circulation in blood vessels, by combining the physical techniques here with chemical methods to label specific cells or biological targets with these types of nanoparticle probes[34]. Our technique also allows to obtain a multicolor image of more than two different nanoparticle probes by switching the excitation wavelength between their resonance wavelengths, if the resonance peaks of the nanoparticle probes are sufficiently separated. The capability of multicolor imaging expands application of our technique to multi-target observation in deep tissue.

Acknowledgement

This work was supported by Japan Society for the Promotion of Science (JSPS) Core-to-Core Program,

This work was supported by the Outstanding Young Scholarship Project of Ministry of Science and Technology (MOST), Taiwan, under grant MOST-105-2628-M-002-010-MY4 and MOST-108-2321-B-002-058-MY2, as well as supported by the Higher Education Sprout Project funded by MOST and the Ministry of Education in Taiwan.

Supporting Information

Supporting Information Available: <Section 1: Dependence of the demodulated scattering signal from the gold nanoshells on the excitation wavelength, Section 2: Detection of 3rd order nonlinear signal from gold nanoshells>

This material is available free of charge vie the Internet at http://pubs.acs.org

References

1. Ntziachristos, V. Going deeper than microscopy: The optical imaging frontier in biology. *Nat. Methods* **2010**, 7, 603–614.
2. Helmchen, F.; Denk, W. Deep tissue two-photon microscopy. *Nat. Methods* **2005**, 2, 932–940.
3. Denk, W.; Strickler, J.; Webb, W. Two-photon laser scanning fluorescence microscopy. *Science.* **1990**, 248, 73–76.
4. Gannaway, J. N.; Sheppard, C. J. R. Second-harmonic imaging in the scanning optical microscope. *Opt. Quantum Electron.* **1978**, 10, 435–439.
5. Freund, I.; Deutsch, M. Second-harmonic microscopy of biological tissue. *Opt. Lett.* **1986**, 11, 94-96.
6. Yamanaka, M.; Yonemaru, Y.; Kawano, S.; Uegaki, K.; Smith, N. I.; Kawata, S.; Fujita, K. Saturated excitation microscopy for sub-diffraction-limited imaging of cell clusters. *J. Biomed. Opt.* **2013**, 18, 126002.
7. Zipfel, W. R.; Williams, R. M.; Webb, W. W. Nonlinear magic: Multiphoton microscopy in the biosciences. *Nat. Biotechnol.* **2003**, 21, 1369–1377.
8. Chu, S.; Su, T.; Oketani, R.; Huang, Y.; Wu, H.; Yonemaru, Y.; Yamanaka, M.; Lee, H.; Zhuo, G.; Lee, M.; Kawata, S.; Fujita, K. Measurement of a Saturated Emission of Optical Radiation from Gold Nanoparticles : Application to an

Ultrahigh Resolution Microscope. **2014**, 112, 017402.

9. Chu, S. W.; Wu, H. Y.; Huang, Y. T.; Su, T. Y.; Lee, H.; Yonemaru, Y.; Yamanaka, M.; Oketani, R.; Kawata, S.; Shoji, S.; Fujita, K. Saturation and Reverse Saturation of Scattering in a Single Plasmonic Nanoparticle. *ACS Photonics* **2014**, 1, 32–37.
10. Deka, G.; Nishida, K.; Mochizuki, K.; Ding, H. X.; Fujita, K.; Chu, S. W. Resolution enhancement in deep-tissue nanoparticle imaging based on plasmonic saturated excitation microscopy. *APL Photonics* **2018**, 3, 031301.
11. Fujita, K.; Kobayashi, M.; Kawano, S.; Yamanaka, M.; Kawata, S. High-Resolution Confocal Microscopy by Saturated Excitation of Fluorescence. **2007**, 99, 228105.
12. Lee, H.; Oketani, R.; Huang, Y.; Li, K.; Yonemaru, Y.; Yamanaka, M.; Kawata, S.; Fujita, K.; Chu, S. Point spread function analysis with saturable and reverse saturable scattering. **2014**, 22, 26016-26022.
13. Jain, P. K.; Lee, K. S.; El-Sayed, I. H.; El-Sayed, M. A. Calculated absorption and scattering properties of gold nanoparticles of different size, shape, and composition: Applications in biological imaging and biomedicine. *J. Phys. Chem. B* **2006**, 110, 7238–7248.
14. Sokolov, K.; Follen, M.; Aaron, J.; Pavlova, I.; Malpica, A.; Lotan, R.; Richards-Kortum, R. Real-time vital optical imaging of precancer using anti-epidermal growth factor receptor antibodies conjugated to gold nanoparticles. *Cancer Res.* **2003**, 63, 1999–2004.
15. Qian, W.; Huang, X.; Kang, B.; El-Sayed, M. A. Dark-field light scattering imaging of living cancer cell component from birth through division using bioconjugated gold nanoprobes. *J. Biomed. Opt.* **2010**, 15, 046025.
16. Smith, A. M.; Mancini, M. C.; Nie, S. Bioimaging: Second window for in vivo imaging. *Nat. Nanotechnol.* **2009**, 4, 710–711.
17. Yu, Y. Y.; Chang, S. S.; Lee, C. L.; Wang, C. R. C. Gold nanorods: electrochemical synthesis and optical properties. *J. Phys. Chem. B* **1997**, 101, 6661–6664.
18. Oldenburg, S. J.; Averitt, R. D.; Westcott, S. L.; Halas, N. J. Nanoengineering of optical resonances. *Chemical Physics Chem. Phys.* **1998**, 288, 243–247.
19. Chen, Y. T.; Lee, P. H.; Shen, P. T.; Launer, J.; Oketani, R.; Li, K. Y.; Huang, Y. T.; Masui, K.; Shoji, S.; Fujita, K.; Chu, S. W. Study of Nonlinear Plasmonic Scattering in Metallic Nanoparticles. *ACS Photonics* **2016**, 3, 1432–1439.

20. Oldenburg, S. J.; Jackson, J. B.; Westcott, S. L.; Halas, N. J. Infrared extinction properties of gold nanoshells. *Appl. Phys. Lett.* **1999**, 75, 2897–2899.
21. Pu, Y.; Shi, L.; Pratavieira, S.; Alfano, R. R. Two-photon excitation microscopy using the second singlet state of fluorescent agents within the 'tissue optical window'. *J. Appl. Phys.* **2013**, 114, 153102.
22. Cubeddu, R.; Pifferi, A.; Taroni, P.; Torricelli, A.; Valentini, G. A solid tissue phantom for photon migration studies. *Phys. Med. Biol.* **1997**, 42, 1971–1979.
23. Di Ninni, P.; Bérubé-Lauzière, Y.; Mercatelli, L.; Sani, E.; Martelli, F. Fat emulsions as diffusive reference standards for tissue simulating phantoms?. *Appl. Opt.* **2012**, 51, 7176-7182.
24. Sivan, Y.; Chu, S. W. Nonlinear plasmonics at high temperatures. *Nanophotonics* **2017**, 6, 317–328.
25. Mulvaney, P. Not All That's Gold Does Glitter. *MRS Bull* **2001**, 26, 1009-1014.
26. Guo, Z.; Park, S.; Yoon, J.; Shin, I. Recent progress in the development of near-infrared fluorescent probes for bioimaging applications. *Chem. Soc. Rev.* **2014**, 43, 16–29.
27. Kim, S.; Lim, Y. T.; Soltesz, E. G.; De Grand, A. M.; Lee, J.; Nakayama, A.; Parker, J. A.; Mihaljevic, T.; Laurence, R. G.; Dor, D. M.; Cohn, L. H.; Bawendi, M. G.; Frangioni, J. V. Near-infrared fluorescent type II quantum dots for sentinel lymph node mapping. *Nat. Biotechnol.* **2004**, 22, 93–97.
28. Welsher, K.; Sherlock, S. P.; Dai, H. Deep-tissue anatomical imaging of mice using carbon nanotube fluorophores in the second near-infrared window. *Proc. Natl. Acad. Sci.* **2011**, 108, 8943–8948.
29. Oketani, R.; Doi, A.; Smith, N. I.; Nawa, Y.; Kawata, S.; Fujita, K. Saturated two-photon excitation fluorescence microscopy with core-ring illumination. *Opt. Lett.* **2017**, 42, 571-574.
30. Nawa, Y.; Yonemaru, Y.; Kasai, A.; Oketani, R.; Hashimoto, H.; Smith, N. I.; Fujita, K. Saturated excitation microscopy using differential excitation for efficient detection of nonlinear fluorescence signals. *APL Photonics* **2018**, 3, 080805.
31. Yonemaru, Y.; Palonpon, A. F.; Kawano, S.; Smith, N. I.; Kawata, S.; Fujita, K. Super-spatial- and -spectral-resolution in vibrational imaging via saturated coherent anti-stokes Raman scattering. *Phys. Rev. Appl.* **2015**, 4, 014010.
32. Gong, L.; Zheng, W.; Ma, Y.; Huang, Z. Saturated Stimulated-Raman-Scattering

Microscopy for Far-Field Superresolution Vibrational Imaging. *Phys. Rev. Appl.* **2019**, 11, 034041.

33. Gu, Y.; Cheong, K. L.; Du, H. Modification and comparison of three Gracilaria spp. agarose with methylation for promotion of its gelling properties. *Chem. Cent. J.* **2017**, 11, 1–10.
34. El-Sayed, I. H.; Huang, X.; El-Sayed, M. A. Surface plasmon resonance scattering and absorption of anti-EGFR antibody conjugated gold nanoparticles in cancer diagnostics: Applications in oral cancer. *Nano Lett.* **2005**, 5, 829–834.

For Table of Contents Use Only

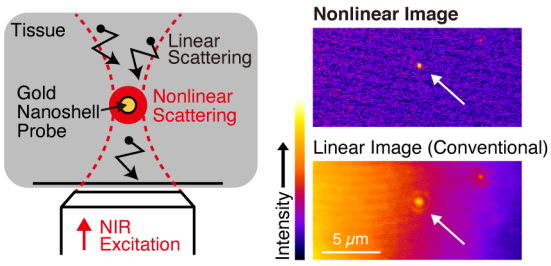

Manuscript title:

Nonlinear scattering of near-infrared light for imaging plasmonic nanoparticles in deep tissue

Names of authors:

Kentaro Nishida, Gitanjal Deka, Nicholas Isaac Smith, Shi-Wei Chu, and Katsumasa Fujita

Brief synopsis describing the graphic:

We utilized the nonlinearity of near-infrared scattering from gold nanoshells for high-contrast imaging of nanoparticles in deep tissue. The nonlinear relation between the illumination laser and the saturated scattering at a gold nanoshell was used to separate the signal and the background light from the tissue. The technique allows us to image gold nanoshell probes in tissue by using near-infrared light for both illumination and detection.